Electronic Supplementary Material (ESI) for Inorganic Chemistry Frontiers.

Controllable fabrication of a nickel-iridium alloy network by galvanic replacement engineering for high-efficiency electrocatalytic water splitting

Su Yan,[a] Mengxiao Zhong,[a] Wendong Zhu,[a] Weimo Li,[a] Xiaojie Chen,[a] Meixuan Li,*[b] Ce Wang[a] and Xiaofeng Lu *[a]

[a] *Alan G. MacDiarmid Institute, College of Chemistry, Jilin University, Changchun 130012, P.R. China*

E-mail: xflu@jlu.edu.cn

[b] *Key Laboratory of Automobile Materials of Ministry of Education & School of Materials Science and Engineering, Nanling Campus, Jilin University, No. 5988 Renmin Street, Changchun 130025, P.R. China*

Email: limeixuan@jlu.edu.cn

Experimental section

Materials. Iridium (III) chloride hydrate ($IrCl_3 \cdot xH_2O$) and commercial iridium oxide (IrO_2) were obtained from Aladdin. Sodium borohydride ($NaBH_4$) was provided by Xilong Scientific Co., Ltd. Nickel (II) chloride hexahydrate ($NiCl_2 \cdot 6H_2O$) was obtained from Tianjin Yongsheng Fine Chemical Co., Ltd. The Nafion 117 dispersion was bought from Sigma-Aldrich. The commercial 20 wt% Pt/C was provided by Johnson Matthey.

Preparation of the Ni network. First, Ni hydrogel was synthesized by an *in situ* spontaneous gelation procedure using a one-step $NaBH_4$ reduction approach. 0.1188 g of $NiCl_2 \cdot 6H_2O$ was dissolved in 10 mL of deionized water. Fresh $NaBH_4$ aqueous solution (0.0568 g of $NaBH_4$ was dissolved in 15 mL of deionized water) was rapidly injected into $NiCl_2$ aqueous solution. Then the mixed solution was reacted at room temperature for 3 h to obtain the Ni hydrogel. The as-prepared Ni hydrogel was washed with deionized water for several times and then freeze-dried overnight.

Preparation of the Ni-Ir0.25, Ni-Ir0.5 and Ni-Ir1.0 network catalysts. 2 mg of the as-synthesized Ni network and 0.5 mL of $IrCl_3$ aqueous solution (10 mg mL^{-1}) were added to 5 mL of deionized water. The mixed solution was sonicated for several seconds and then transferred into an oil bath at 80 ℃. After 4 h, the aggregated sample (denoted as Ni-Ir0.5) was collected by centrifugation, rinsed for five times with deionized water, and freeze-dried overnight. Similarly, the Ni-Ir0.25 and Ni-Ir1.0 catalysts were fabricated by the same preparation procedure, except for different volumes with $IrCl_3$ solution: Ni-Ir0.25 (0.25 mL of 10 mg mL^{-1} $IrCl_3$ aqueous solution) and Ni-Ir1.0 (1.0 mL of 10 mg mL^{-1} $IrCl_3$ aqueous solution). In the three samples of Ni-Ir0.25, Ni-Ir0.5 and Ni-Ir1.0, the feeding molar ratios between Ni network and $IrCl_3$ are calculated to be around 4:1, 2:1 and 1:1, respectively.

Preparation of the Ni network-2. The Ni network-2 fabricated and obtained with the same fabrication procedure of Ni network except for the freeze-drying process, instead of washing with ethanol for several times and then drying under 45 ℃ in the oven overnight.

Preparation of the Ni-Ir0.5 network-2. 2 mg of the as-synthesized Ni network-2 and 0.5 mL of $IrCl_3$ aqueous solution (10 mg mL^{-1}) were added to 5 mL of deionized water. The mixed solution was sonicated for several seconds and then transferred into an oil bath at 80 ℃. After 4 h, the aggregated sample (denoted as Ni-Ir0.5 network-2) washed with ethanol for several times and then drying under 45 ℃ in the oven overnight.

Material characterization. The morphologies of all the resultant network samples were characterized by the field-emission scanning electron microscope (FESEM, FEI Nova NanoSEM). High-resolution TEM (HRTEM) images, energy dispersive X-ray (EDX) spectrum and corresponding elemental maps were gained from an FEI Tecnai G2 F20 electron microscope with an operating voltage of 200 kV. The crystallographic structure of the samples was investigated by X-ray diffraction (XRD, PANalytical B.V. Empyrean) with Cu Kα radiation. X-ray photoelectron spectroscopy (XPS) was conducted on a Thermo Scientific ESCALAB250 system. The Brunauer-Emmett-Teller (BET) specific surface area was determined using N_2 adsorption-desorption on a Micromeritics ASAP 2020 PLUS instrument with started temperature hold at 200 ℃.

Electrochemical measurements. All electrochemical tests were performed on a CHI660E electrochemistry workstation. The preparation process of the working electrode is as follows: 4 mg of catalyst was dispersed into the mixture of deionized water (490 μL), ethanol (490 μL) and Nafion (20 μL) under vigorously ultrasonication until fully dispersed. Afterward, the above suspension (50 μL) was loaded on carbon paper (covered area: 0.196 cm^2) and dried at room temperature. The mass loading of the as-prepared catalysts, commercial IrO_2 and 20% Pt/C was around 1.0 mg cm^{-2} in all electrochemical tests. For the HER and OER measurements, a standard three-electrode system was employed, in which mercury oxide (Hg/HgO) was selected as the reference electrode, and a carbon rod and a Pt wire were used as the counter electrodes for HER and OER, respectively. All the linear sweep voltammetry (LSV) curves were carried out with a scan rate of 1 mV s^{-1} with *iR*-compensation. The CV cycle stability measurements were performed at -0.8 V to -1.2 V and 0.4 V to 0.8 V (vs. Hg/HgO) for HER and OER, respectively, with a scan rate of 100 mV s^{-1}. The procedure for

calibrating the Hg/HgO reference electrode was as follows. Two platinum plates were used as the working electrode and counter electrode and then a CV measurement with two sweep segments was carried out in hydrogen-saturated 1 M KOH electrolyte with a scan rate of 1 mV s^{-1}. The average of two potentials at which the current crossed zero was recorded to be the thermodynamic potential for the hydrogen electrode reaction. As displayed in **Fig. S15**, the average value of two zero current potentials was -0.932 V. The potentials were calculated to a reversible hydrogen electrode (RHE) in terms of the following equation: $E_{RHE} = E_{Hg/HgO} + 0.932$. The electrochemical impedance spectroscopy (EIS) tests for Fig. 3f were performed at $E_{Hg/HgO}$ of -0.95 V from 10^5 to 0.1 Hz. The mass activity (MA) values of HER and OER were computed at overpotentials of 100 and 300 mV by the equation (MA = j/m), respectively, in which j is the current density (mA cm^{-2}) at a definite overpotential and m is the mass loading (mg cm^{-2}) of the as-prepared electrocatalysts. The values of double layer capacitance (C_{dl}) of different samples were calculated in terms of capacitive current density ($\Delta j/2 = (j_a - j_c)/2$) at different scan rates under non-Faraday interval. The electrochemically active surface area (ECSA) of all samples were acquired based on the equation (ECSA = $C_{dl}/C_s \times L$), where the value of C_s is assumed to be 40 μF cm^{-2} and L is the mass loading of the catalyst.

For the overall electrolysis water measurement, a typical two-electrode configuration was performed, where the Ni-Ir0.5 catalyst loaded on carbon papers were used as both cathode and anode. LSV for the overall electrolysis water was measured under 1 mV s^{-1} without *iR*-compensation. The mass loading of catalyst for the overall electrolysis water is the same as the previous HER and OER tests.

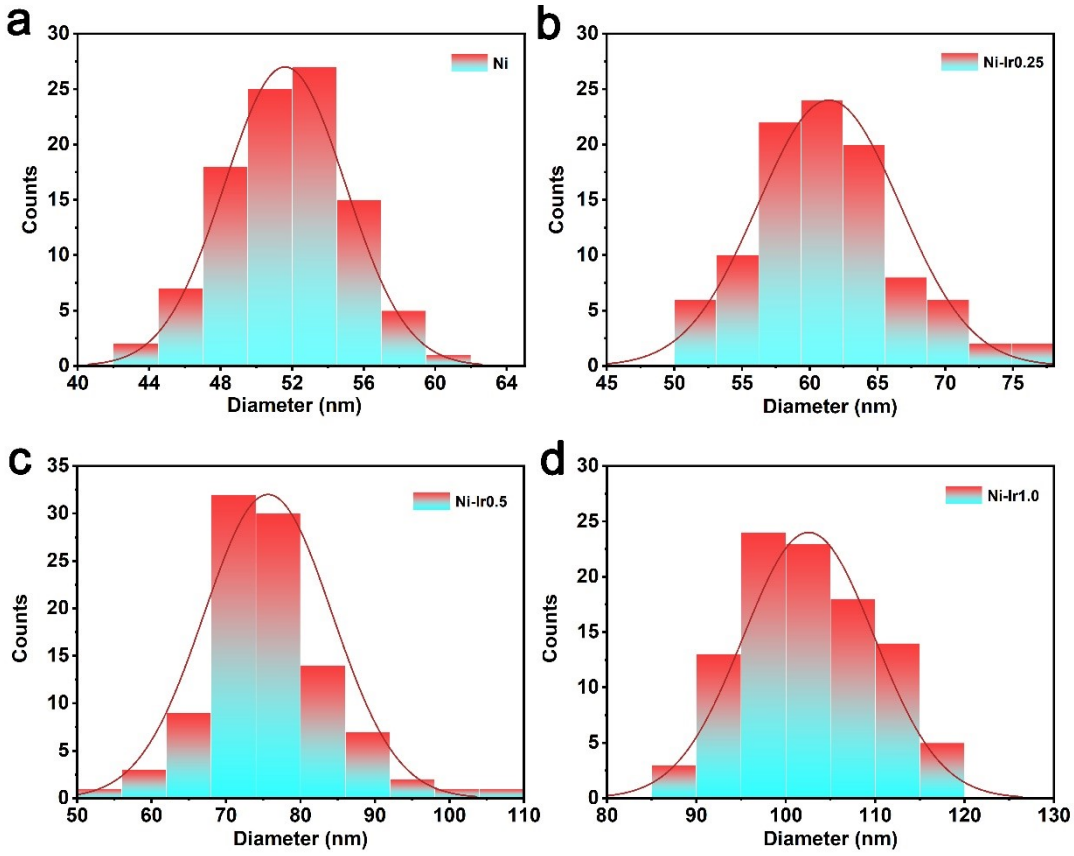

Fig. S1. The diameter distribution of nanoparticles in a-d) Ni, Ni-Ir0.25, Ni-Ir0.5 and Ni-Ir1.0. The average diameters are 51.6 nm, 61.4 nm, 75.7 nm and 102.6 nm, respectively.

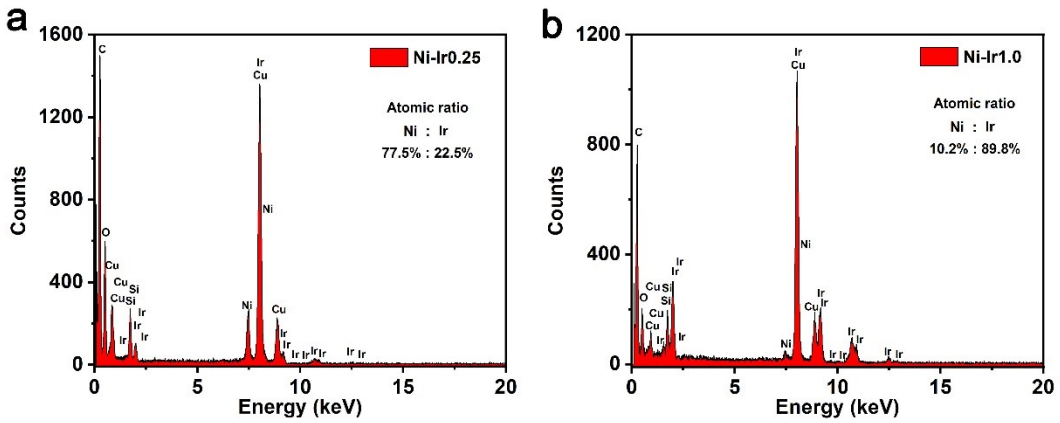

Fig. S2. a-b) EDX spectra of Ni-Ir0.25 and Ni-Ir1.0.

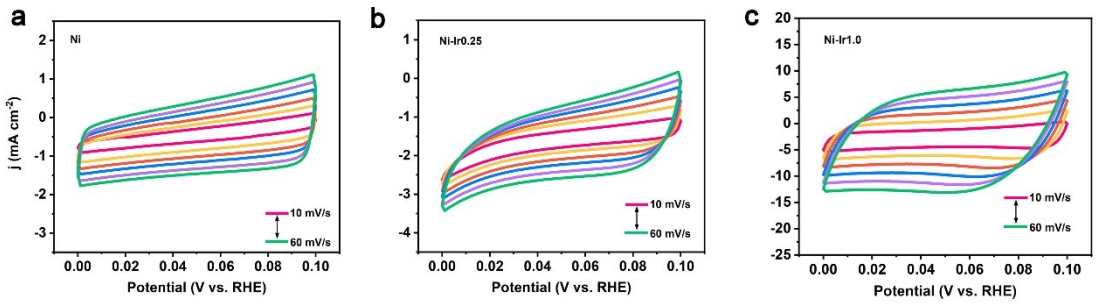

Fig. S3. CV curves at different scan rates (10-60 mV/s) for (a) Ni, (b) Ni-Ir0.25 and (c) Ni-Ir1.0.

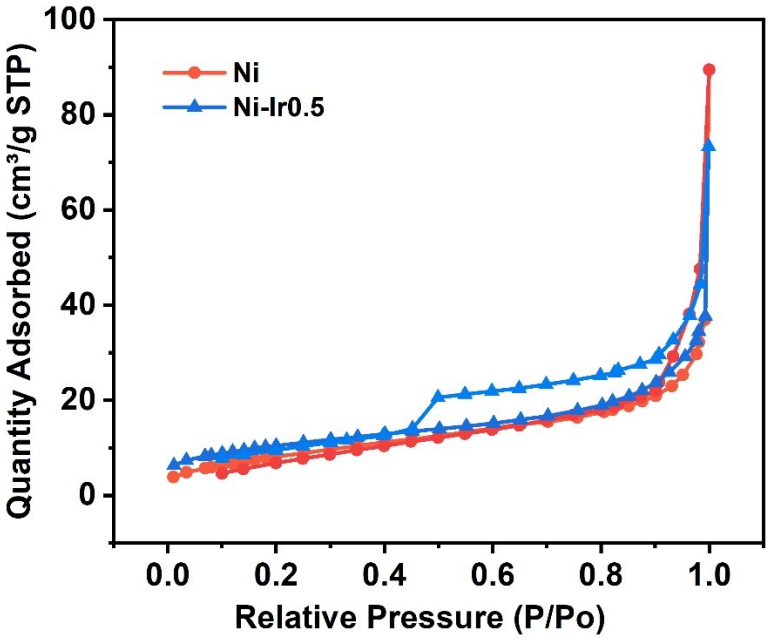

Fig. S4. Nitrogen adsorption/desorption isotherms of Ni and Ni-Ir0.5 samples.

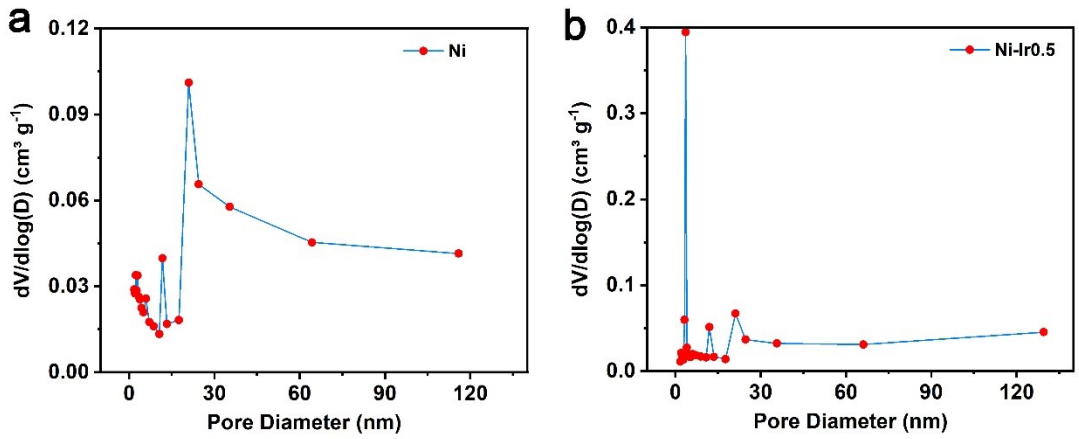

Fig. S5. The pore size distribution of Ni and Ni-Ir0.5 samples.

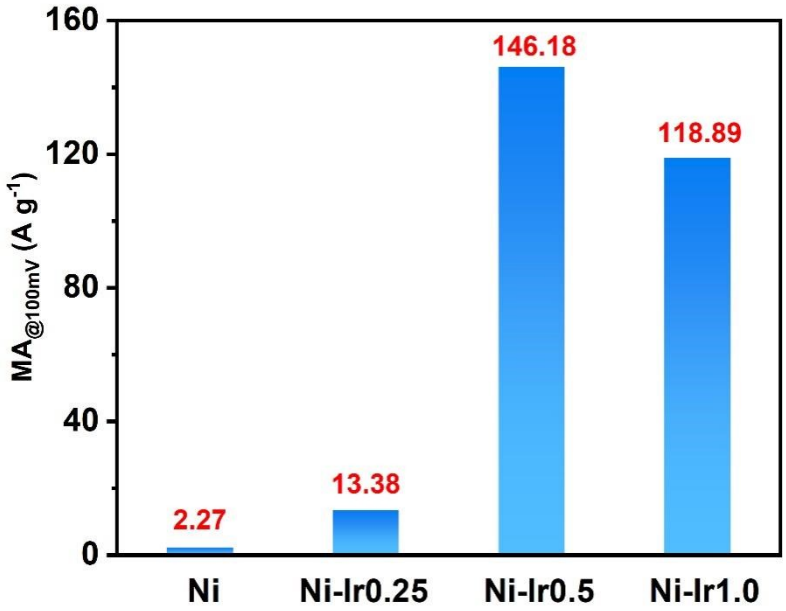

Fig. S6. The mass activity at the overpotential of 100 mV for as-prepared catalysts during HER process in 1 M KOH.

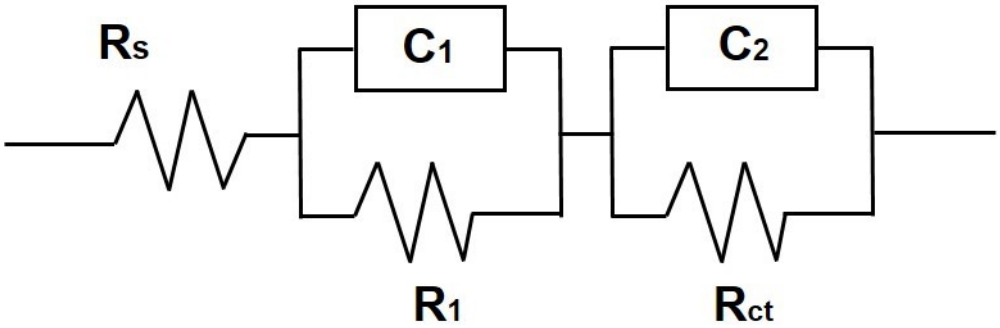

Fig. S7. The equivalent circuit model used for simulating the Nyquist plots.

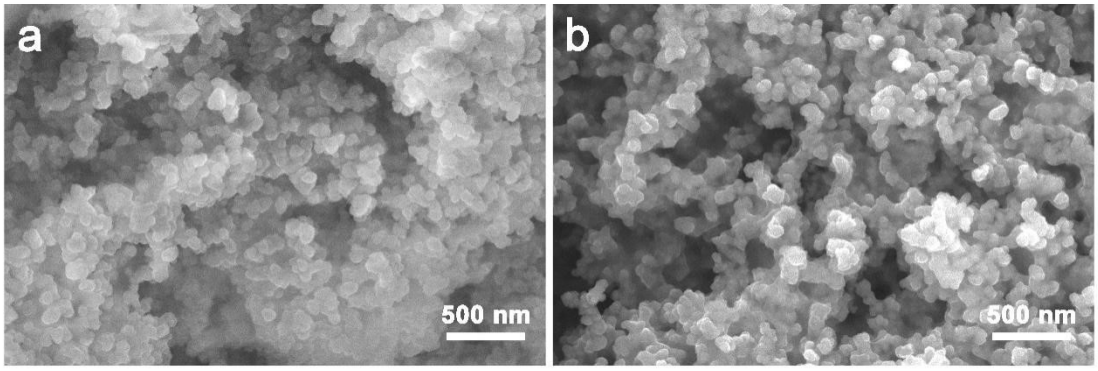

Fig. S8. SEM images of Ni-Ir0.5 after stability tests: (a) HER and (b) OER.

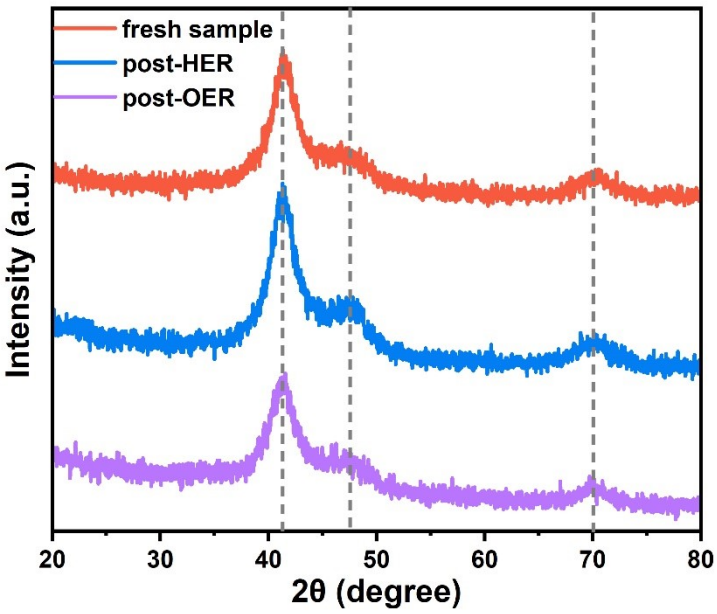

Fig. S9. XRD patterns of Ni-Ir0.5 before and after stability tests.

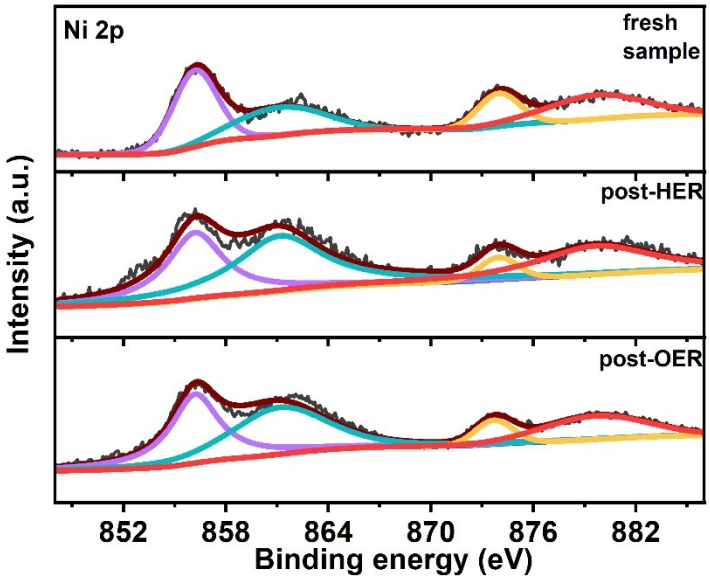

Fig. S10. Ni 2p spectra of Ni-Ir0.5 before and after stability tests.

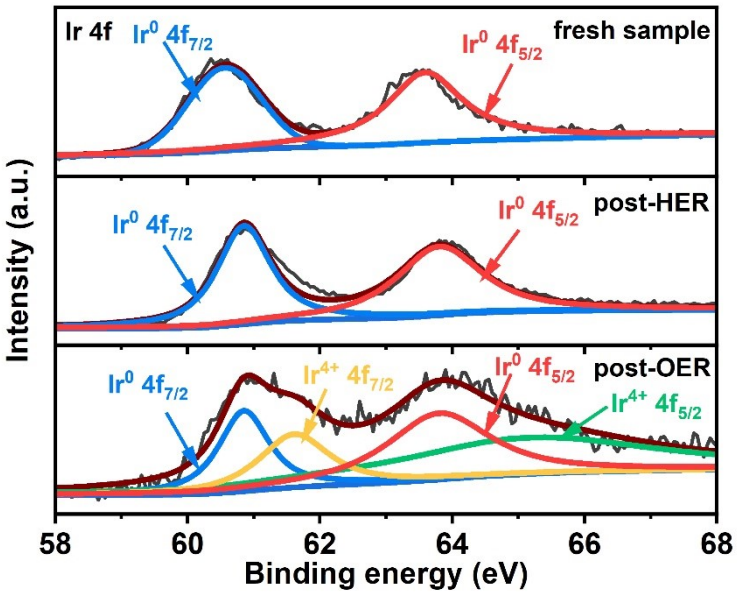

Fig. S11. Ir 4f spectra of Ni-Ir0.5 before and after stability tests.

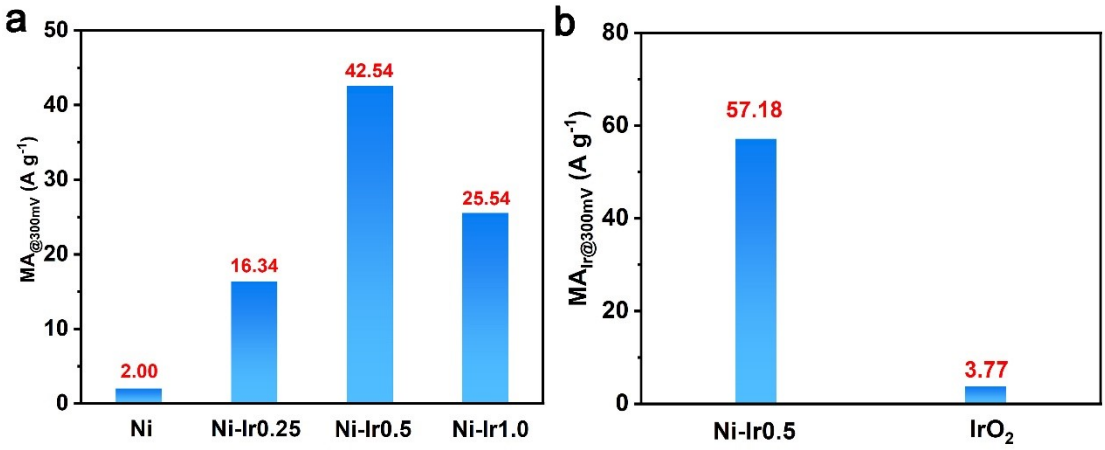

Fig. S12. a) The MA at the overpotential of 300 mV for as-prepared catalysts during OER process, b) the comparison of MA_{Ir} between Ni-Ir0.5 and commercial IrO_2 at the overpotential of 300 mV during OER process.

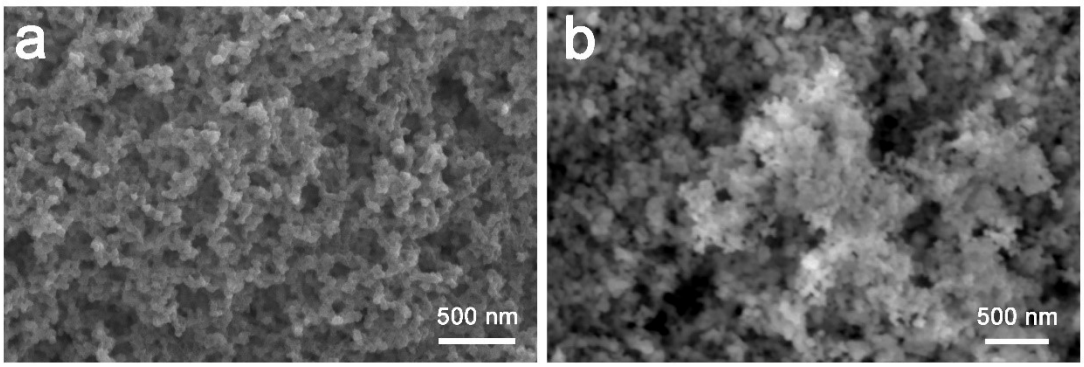

Fig S13. (a-b) The images of Ni network-2 and Ni-Ir0.5 network-2.

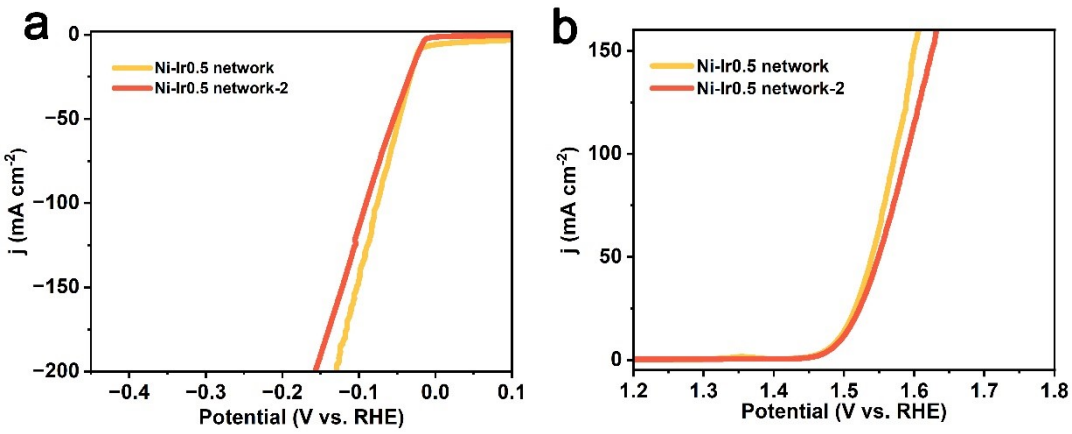

Fig S14. (a-b) HER and OER LSV curves of Ni-Ir0.5 network and Ni-Ir0.5 network-2.

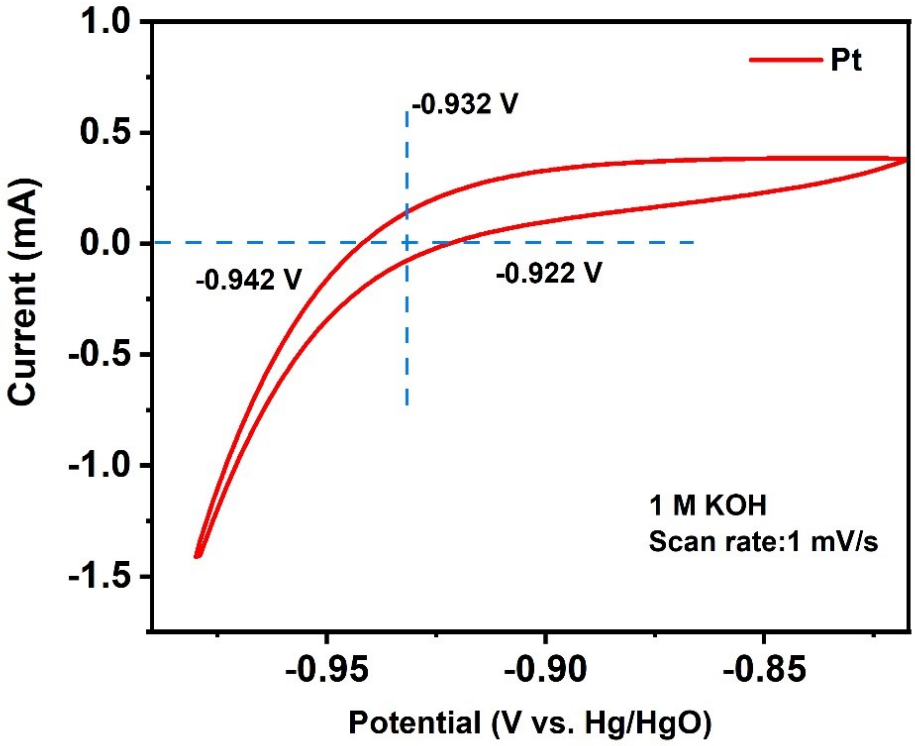

Fig. S15. RHE voltage calibration.

Table S1. Comparison of the HER performance for Ni-Ir0.5 catalyst with other electrocatalysts in alkaline solution.

Catalyst	Electrolyte	η_{10} [mV]	Tafel slope [mV dec^{-1}]	Reference
Ni-Ir0.5	1 M KOH	22	29.4	This work
Ru_1CoP/CDs	1 M KOH	51	47	Angew. Chem. Int. Ed. 2021, 60, 7234
$N,Pt\text{-}MoS_2$	1 M KOH	38	39	Energy Environ. Sci. 2022, 15, 1201
$RuCoO_x$	1 M KOH	37	53.2	Nano Lett. 2021, 21, 9633
Sr_2RuO_4	1 M KOH	61	51	Nat. Commun. 2019, 10, 149
Ru-30	1 M KOH	36	35	Appl. Catal. B: Environ. 2022, 307, 121199
$Ni/Mo_2C(1:2)\text{-}NCNFs$	1 M KOH	143	57.8	Adv. Energy Mater. 2019, 1803185
RuNi-NCNFs	1 M KOH	35	30	Adv. Sci. 2020, 7, 1901833
CDs/Pt-PANI	1 M KOH	56	41.7	Appl. Catal. B: Environ. 2019, 257, 117905
$IrP_2@NC$	1 M KOH	28	50	Energy Environ. Sci. 2019, 12, 952
RuAu-0.2	1 M KOH	24	37	Adv. Energy Mater. 2019, 9, 1803913
$Ni/CeO_2@N\text{-}CNFs$	1 M KOH	32	85.7	Small 2022, 2106592
Au-Ru-2 NWs	1 M KOH	50	30.8	Nat. Chem. 2018, 10, 456
$RuP_2@NPC$	1 M KOH	52	69	Angew. Chem. Int. Ed. 2017, 56, 11559
$Ni_5P_4\text{-}Ru/CC$	1 M KOH	54	52	Adv. Mater., 2020, 32, 1906972
$\beta\text{-}Ni(OH)_2/Pt$	1 M KOH	115	42	ACS Energy Lett. 2018, 3, 237
$Ru–NiSe_2/NF$	1 M KOH	59	72.2	Small 2021, 2105305
$IrNi\text{-}FeNi_3/NF$	1 M KOH	31.1	36.01	Appl. Catal. B: Environ. 2021, 286, 119881

Table S2. Summary for ECSA values of as-prepared catalysts.

Catalyst	ECSA (m^2 g^{-1})
Ni	38.25
Ni-Ir0.25	36.00
Ni-Ir0.5	434.75
Ni-Ir1.0	402.75

Table S3. Summary of BET surface area among of Ni and Ni-Ir0.5.

Catalyst	BET surface area (m^2 g^{-1})
Ni	31.5
Ni-Ir0.5	37.4

Table S4. Comparison of the OER performance for Ni-Ir0.5 catalyst with other electrocatalysts in alkaline solution.

Catalyst	Electrolyte	η_{10} [mV]	Reference
Ni-Ir0.5	1 M KOH	257	This work
Ir	1 M KOH	430	J. Am. Chem. Soc. 2015, 137, 4347
Exfoliated NiFe LDH	1 M KOH	302	Nat. Commun. 2014, 5, 4477
Ni/Mo_2C(1:2)-NCNFs	1 M KOH	288	Adv. Energy Mater. 2019, 1803185
Ru_3Ni_3 NAs	1 M KOH	304	iScience 2019, 11, 492
Co-Ni_3N	1 M KOH	307	Adv. Mater. 2018, 30, 1705516
Ni_3FeN/r-GO-20	1 M KOH	270	ACS Nano 2018, 12, 245
Co/β-Mo_2C@N-CNTs	1 M KOH	356	Angew.Chem. Int. Ed. 2019, 58, 4923
CoNi-Fe_3N	1 M KOH	285	Small 2020, 16, 2003824
Ru	1 M KOH	320	J. Am. Chem. Soc. 2013, 135, 16977
Ir_3Ni_2/BMNC	1 M KOH	279	Adv. Mater. Interfaces 2020, 2001145
NiMo-PVP/NiFe-PVP	1 M KOH	297	Adv. Energy Mater. 2017, 1700220.
Ru-RuP_x-Co_xP	0.1 M KOH	291	Nano Energy 2018, 53, 270
RuNi-NCNFs	1 M KOH	290	Adv. Sci. 2020, 7, 1901833
FeCoNi-2	1 M KOH	288	ACS Catal. 2017, 7, 469
FeCo-Co_4N/N-C	1 M KOH	280	Adv. Mater. 2017, 29, 1704091

Table S5. Comparison of the overall water splitting performance for Ni-Ir0.5 catalyst with other electrocatalysts in alkaline solution.

Catalyst	Electrolyte	Cell voltage (at 10 mA cm^{-2})	Reference
Ni-Ir0.5	1 M KOH	1.516 V	This work
Pt-CoS_2	1 M KOH	1.550 V	Adv. Energy Mater. 2018, 8, 1800935
Ru-NiCoP/NF	1 M KOH	1.515 V	Appl. Catal. B-Environ. 2020, 279, 119396
Ni_3FeN/r-GO-20	1 M KOH	1.60 V	ACS Nano 2018, 12, 245
Ni/Mo_2C(1:2)-NCNFs	1 M KOH	1.64 V	Adv. Energy Mater. 2019, 9, 1803185
RuNi-NCNFs	1 M KOH	1.564 V	Adv. Sci. 2020, 7, 1901833
NiFeRu-LDH	1 M KOH	1.52 V	Adv. Mater. 2018, 30, 1706279
Ru-HPC/porous RuO_2	1 M KOH	1.53 V	Nano Energy 2019, 58, 1
Co/β-Mo_2C@N-CNTs	1 M KOH	1.64 V	Angew. Chem. Int. Ed. 2019, 58, 4923
$RuTe_2$	1 M KOH	1.57 V	Appl. Catal. B-Environ. 2020, 278, 119281
RuCo NSs	1 M KOH	1.524 V	Adv. Energy Mater. 2018, 2002860
Ni/CeO_2@N-CNFs	1 M KOH	1.56 V	Small 2022, 2106592
Pt-Cu@CuxO NWs-3DF	0.1 M KOH	1.56 V	Nano Energy 2019, 59, 216
NCP/GNS	1 M KOH	1.61 V	Nano Energy 2018, 48, 284
FeIr/NF	1 M KOH	1.51 V	Chem. Eng. J. 2021, 421, 129892
Co@IC/MoC@PC	1 M KOH	1.57V	ACS Nano 2021, 15, 13399
Ir-16-PdCu/C	1 M KOH	1.63 V	Nano Lett. 2021, 21, 13
Ni_3S_2	1 M KOH	1.71 V	J. Am. Chem. Soc. 2015, 137, 14023

NiFe/$NiCo_2O_4$/Ni Foam	**1 M KOH**	**1.67 V**	**Adv. Funct. Mater. 2016, 26, 3515.**
Co_2B	**1 M KOH**	**1.81 V**	**Adv. Energy Mater. 2016, 6, 1502313**